Check for updates

View Article Online
View Journal

NJC
New Journal of Chemistry
A journal for new directions in chemistry

Accepted Manuscript

This article can be cited before page numbers have been issued, to do this please use: T. Soganci, Y. Baygu, N. Kabay, G. Dumlu, Y. Gök and M. Ak, *New J. Chem.*, 2020, DOI: 10.1039/D0NJ03931D.

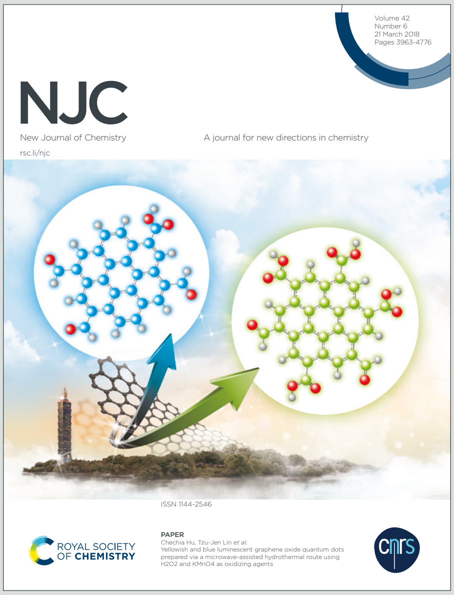

Volume 42
Number 6
21 March 2018
Pages 3963-4776

NJC
New Journal of Chemistry
A journal for new directions in chemistry
rsc.li/njc

ISSN 1144-2546

ROYAL SOCIETY OF CHEMISTRY

PAPER
Chechia Hu, Tzu-Jen Lin *et al.*
Yellowish and blue luminescent graphene oxide quantum dots prepared via a microwave-assisted hydrothermal route using H2O2 and KMnO4 as oxidizing agents

cnrs

This is an Accepted Manuscript, which has been through the Royal Society of Chemistry peer review process and has been accepted for publication.

Accepted Manuscripts are published online shortly after acceptance, before technical editing, formatting and proof reading. Using this free service, authors can make their results available to the community, in citable form, before we publish the edited article. We will replace this Accepted Manuscript with the edited and formatted Advance Article as soon as it is available.

You can find more information about Accepted Manuscripts in the Information for Authors.

Please note that technical editing may introduce minor changes to the text and/or graphics, which may alter content. The journal's standard Terms & Conditions and the Ethical guidelines still apply. In no event shall the Royal Society of Chemistry be held responsible for any errors or omissions in this Accepted Manuscript or any consequences arising from the use of any information it contains.

ROYAL SOCIETY OF CHEMISTRY

rsc.li/njc

View Article Online
DOI: 10.1039/D0NJ03931D

ARTICLE

Received 00th January 20xx,
Accepted 00th January 20xx

DOI: 10.1039/x0xx00000x

Synthesis of carbazole substituted unusual cobalt(II)dioxime complex to design conducting polymer with caged metal centers for enhanced optical and electrical properties

Tugba Soganci[a], Yasemin Baygu[b], Nilgün Kabay[c], Gökhan Dumlu[d], Yaşar Gök[d], Metin Ak[a]*

Conjugated hybrid structures (conductive metallopolymers) designed by incorporating transition metals into conductive polymers can increase the properties of both materials and eliminate the disadvantages of materials for final applications to achieve the desired optical and electrical properties. Here in, S,S'-substituted vicinal dithioglyoxime and its mononuclear cobalt(II) complex has been synthesized and this pseudo macrocyclic Co(II) complex has been converted to full macrocycle by replacement of the hydrogen atoms with BF_2^+ moieties which act as strong electron-withdrawing units to enhance stability of the transition metal and to increase solubility of the macrocycle in common organic solvents. After electrochemical polymerization, polycarbazole based conductive metallopolymer with caged metal centers have been achieved. As a consequence of the optical and electrochemical characterization of the unique structure, the highest optical contrast value was obtained among the polycarbazole derivatives in the literature. Electrochemical polymerization and electrochemical properties of the conducting metallopolymer have been also investigated with EQCM studies.

Introduction

Conductive metallopolymers designed by incorporation of transition metals in conductive polymers have the potential to greatly expand the function of conjugated systems[1,2]. These organic-inorganic hybrid structures obtained with a synergistic combination of metals and conducting polymers can increase properties of both materials and eliminate their disadvantages to obtain desired optical and electrical properties of the materials for ultimate applications[3–5]. Therefore, the strong interaction between polymer and metal components creates distinct electro-chemical, photo-chemical and photo-physical properties, which make these conducting polymers potential materials for many applications such as sensors, electroluminescence, nonlinear optics, solar energy conversion and smart devices[6–10]. It is important to note that the tuning of optical and electrical properties of conducting polymer is highly dependent on the nature of the bridging ligand and metal centers. There exists a diverse group of hybrid systems that incorporate transition metals into conducting polymer structures[11–14]. In the literature, conductive metallopolymers have been designed with two different strategies[3]. In the first strategy emphasized as outer sphere arrangement, non-conjugated tethers attach the redox active metal centers to polymerizable monomer units[15–19]. In this strategy, the metal centers involve as a side group in the polymer backbone. In another strategy called inner sphere arrangement, the metal center is located directly on the polymer backbone[20–22]. A variety of ligands such as bipyridyl and salen have been used for incorporation of metals in to conducting polymers[23,24]. Although oximes especially vicinal dioximes have been commonly utilized as ligand for preparation of many metal complex, any study related to a metallopolymer synthesized by using metal complexes of these ligands has not been found in the literature. Vicinal dioximes are amphoteric chelatic ligands due to the presence of mildly acidic hydroxyl and slightly basic azomethine groups that form corrin-type square-planar, square-pyramidal and octahedral complexes with some transition metal cations [25]. The loss of a proton from each dioxime unit further stabilies due to the subsequent intramolecular hydrogen bonds to afford a 14-membered "pseudomacrocycle". Bis(dioximato) metal (II) complexes are basically insoluble in a lot of organic solvents and water because of the formation of strong hydrogen bonds. These kinds of complexes could be easily converted to full macrocycles by replacement of the bridging hydrogen atoms with an electrophilic group such as BF_2^+ moieties [26]. These electrophilic BF_2^+ groups act as a strong electron-withdrawing unit. This formation increased stability of the lower oxidation states of transition metals and solubilities in common organic solvents. BF_2-capped dioxime cobalt complexes are able to catalyze the reduction of strong acids[27]. Because of the high stability of the vicinal dioxime complexes have been extensively used for various purposes, including metal analysis, a non-biological mimic of coenzyme B_{12}, hydrogen production etc[28–35].

---

[a] *Graduate School of Sciences, Department of Advanced Technologies, Eskisehir Technical University, Eskisehir, Turkey*
[b] *Tavas Vocational High School, Pamukkale University, Denizli, Turkey*
[c] *Department of Biomedical Engineering, Technology Faculty, Pamukkale University, Denizli, Turkey*
[d] *Department of Chemical Engineering, Engineering Faculty, Usak University, Uşak, Turkey*

Electronic Supplementary Information (ESI) available: [1H-NMR, 13C-NMR, FTIR and MS spectra of the chemicals are provided in ESI]. See DOI: 10.1039/x0xx00000x

View Article Online
DOI: 10.1039/D0NJ03931D

In this study S,S'-substituted vicinal dithioglyoxime has been synthesized from 6-(9H-carbazol-9-yl)hexane-1-thiol and cyanogen di-N-oxide. Mononuclear cobalt(II) complex of dioxime with a metal:ligand ratio of 1:2 has been isolated and this pseudo macrocyclic Co(II) complex has been converted to full macrocycle by replacement of the hydrogen atoms with BF_2^+ moieties which act as strong electron-withdrawing units to enhance stability of the transition metal and to increase solubility of the macrocycle in common organic solvents. After electrochemical polymerization the first polycarbazole based conductive metallopolymer with caged metal centers have been obtained. As a result of the optical and electrochemical characterization of the unique structure, the highest optical contrast value was obtained among the polycarbazole derivatives in the literature. Electrochemical polymerization and electrochemical properties of the conducting metallopolymer have been also investigated with EQCM studies.

Experimental

Materials and Methods

^1H and ^{13}C NMR spectra were recorded on an Agilent-400 spectrometer using TMS as internal reference. FT-IR and UV-vis spectra were recorded with on a Perkin-Elmer UATR spectrometer and on a Shimadzu UV-1601 spectrometer using 1 cm path length cuvettes at room temperature. Mass spectra were performed on a Bruker MicroTOF ESI/MS or Bruker microflex LT MALDI-TOF spectrometers. Elemental analysis of compounds was determined on a Costech ECS 4010 instrument. Cobalt contents of the complexes have been measured on Perkin–Elmer Analyst 700 Atomic Absorption Spectrometer. Melting points were determined on an electro thermal melting point apparatus in a sealed capillary and are uncorrected. All reagents and solvents were purchased from commercial suppliers and solvents were dried over standard drying agents. (E, E) dichloroglyoxime[36], cyanogen-di-*N*-oxide[37] and 6-(9H-carbazol-9-yl)hexane-1-thiol[19] were prepared according to the reported procedures.

Synthesis

Preparation of S,S'-bis [(6-(9H-carbazol-9-yl)hexane-1]thioglyoxime (H_2L)

A solution of cyanogen di-N-oxide which was prepared by treating a suspension of (E, E)-dichloroglyoxime (0.785 g, 5 mmol) in dichloromethane (50 mL) with aqueous solution of Na2CO3 (25 mL, 0.5 M) at -15 °C was added to a solution of 6-(9H-carbazol-9-yl)hexane-1-thiol (1.132 g, 4 mmol) in dichloromethane under argon atmosphere at the same temperature. The solution was stirred at -15 °C for 24 h, then allowed to warm up to room temperature. The end of this period, the solution was evaporated to 20 mL under reduced pressure and then cooled in a refrigerator at -18 °C overnight, whereupon the product crystallized from the solution. The colorless product was filtered off and dried in vacuum over P_4O_{10}. Yield: 0.48 g (44.61%), m.p: 178 °C (dec.). ^1H NMR (400 MHz, $CDCl_3$) δ: 9.22 (s, 2H, N-OH, D_2O-exchangeable), 8.02-7.99 (d, 4H, Ar-H), 7.38 (d, 4H, Ar-H), 7.31 (m, 4H,Ar-H), 7.14 m, 4H,Ar-H), 4.18 (t, 4H,NCH_2), 2.68 (t, 4H,SCH_2), 1.77 (m, 4H,CH_2), 1.61 (m, 4H,CH_2), 1.46 (m, 4H,CH_2), 1.25 (m, 4H, CH_2) (Figure S1 and Figure S2). ^{13}C NMR (100 MHz, $CDCl_3$) δ: 149.47, 140.60, 125.84, 123.01, 120.60, 118.98, 108.87, 43.07, 31.18, 29.80, 29.01, 28.48, 26.89 (Figure S3). $[M]^+$. Calculated elemental analysis for $C_{38}H_{42}N_4S_2O_2$: C,70.12; H,6.50; N,8.91. Found: C,70.31; H,6.32; N,8.44 MS (ESI) m/z : 650.639 (Figure S4). FT-IR (ATR, cm-1): 3221, 3060, 3008, 2971-2855, 1626, 1594, 1483, 1451, 1326, 1215, 969, 885, 747 (Figure S5).

Preparation of cobalt(II) complex $[Co(HL)_2]$

$CoCl_2.\ 6H_2O$ (0.059 g, 0.25 mmol) in 10 mL absolute ethanol was dropwise added to the 25 mL solution of dioxime (0.325 g, 0.5 mmol) in absolute ethanol stirred at 60 °C under argon atmosphere. A color change and pH decrease of the reaction mixture was observed (pH = 1.01). pH value of the mixture was increased with KOH (0.1 M) in ethanol to pH=4.40 which the complex started to precipitate. After that the mixture was stirred at 65 °C for a further 4 h, and during this period precipitation of complex was completed. The brown product was filtered and washed cold ethanol and then dried under P_4O_{10} in vacuum. Yield: 0.328 g (96.75%), m.p. 242 °C (dec). FT-IR (ATR, cm^{-1}): 3048, 3016, 2927-2851, 1768, 1626, 1595, 1483, 1451, 1324, 1213, 1151, 1120, 1020,1000, 920, 883 (Figure S6). MALDI/TOF (MS) m/z: 648.913 $[M-LH_2-Co]^+$. Calculated elemental analysis for $C_{76}H_{82}N_8S_4O_4Co$: C, 67.18; H, 6.08; N, 8.25; Co, 4.34. Found: C, 67.35; H, 5.88; N, 8.47; Co, 4.58 (Figure S7).

Preparation BF_2^+-capped cobalt(II) complex $[Co(LBF_2)_2]$

Under argon atmosphere 30 mL solution of Cobalt(II) complex (0.271 g, 0.2 mmol) in distilled acetonitrile and dichloromethane mixture (2:1, v,v) was stirred and heated at 45 °C. Boron trifluoride diethyl etherate complex (0.079 g, 0.5 mmol) was dropwise added to this solution, which immediately changed color to red. The mixture was heated and stirred at above temperature for 1h. After removal the solvent under reduced pressure and the crude product was dissolved in 12 mL mixture of acetonitrile and dichloromethane (2:1) and the solvent was removed under reduced pressure. The red crude product was washed with acetonitrile, cold ethanol and then dried over P_4O_{10}. In order to obtain pure brown solid product, the dark brown product was purified by column chromatography [silica gel (THF:hexane)(2:1)]. Yield: 0.21 g (52.41%), m.p. 121 °C dec.). FT-IR (ATR, cm^{-1}): 3049, 3020, 2927-2854, 1625, 1595, 1483, 1462, 1451, 1325, 1218, 1152, 1120, 1061, 1020, 925, 883, 802 (Figure S8). MALDI/TOF (MS) m/z: 1492.275 $[M+K]^+$, 1337.277 $[M-BO_3F_3]^+$. Calculated elemental analysis for $C_{76}H_{80}N_8S_4O_4B_2F_4Co$: C, 62.77; H, 5.54; N, 7.71; Co, 4.05: Found: C, 62.50; H, 5.80; N, 7.99; Co, 3.81 (Figure S9).

View Article Online
DOI: 10.1039/D0NJ03931D

Electrochemical, Spectroelectrochemical and EQCM Studies

All electrochemical processes (electropolymerization and electrochemical characterizations) were performed in a 3 mL electrolysis cell containing three electrodes (Silver wire as reference, Platinum wire as counter and ITO coated glass electrode as working electrode) using Ivium CompactStat Potentiostat. The pseudo reference electrode (Ag wire) was externally calibrated by Fc/Fc$^+$ redox couple. Spectroelectrochemical characterizations of the polymer-coated electrode have been performed by using the potentiostat and UV-vis Spectrophotometer (Agilent HP8356) together. EQCM experiment were collected using a Gamry eQCM 10M instrument coupled with a Gamry Reference 600 potentiostat. Working electrode in EQCM analyses was an Au deposited on 10 MHz quartz crystals.

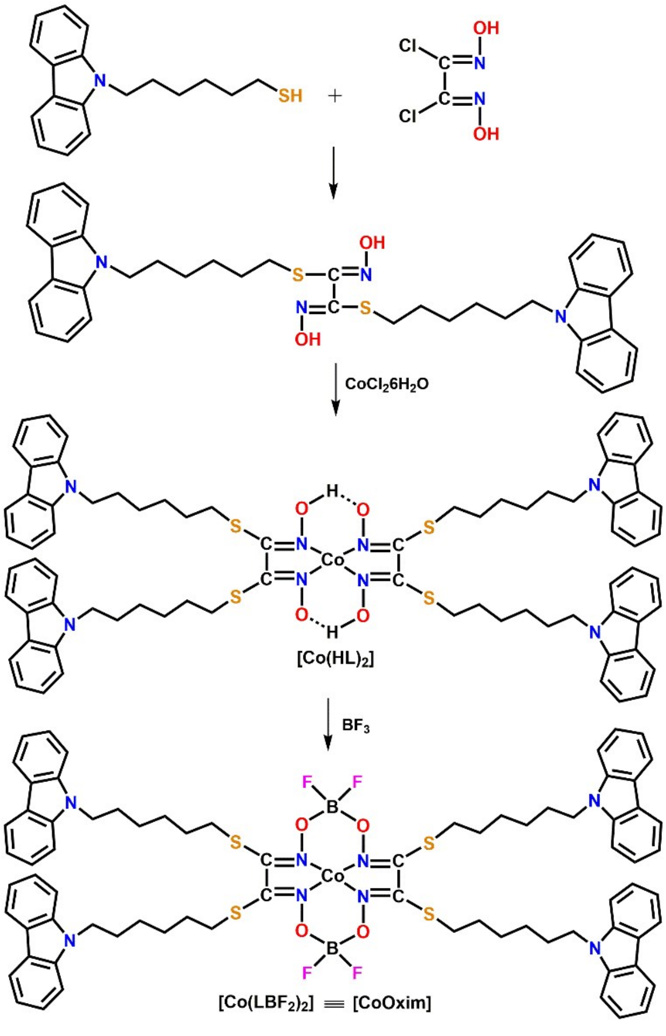

Scheme 1 Synthesis scheme of the CoOxim [Co(LBF2)2]

Preparation of Cobalt Cage Conducting Polymer

Electrochemical studies were performed with potentiodynamic scan (cyclic voltammetry) that were recorded by an Ivium Compactstat potentiostat/galvanostat. The 0.001 mM CoOxim was dissolved in dichloromethane (DCM) containing 0.05 M supporting electrolyte (tetrabutyl ammonium hexafluorophosphat, TBP). A three-electrode containing electrochemical cell was used. In the system a silver wire (calibrated ferrocene-ferrocenium couple) and a platinum wire was used as reference electrode and counter electrode, respectively. Indium-tin-oxide coated glass slide (ITO, 0.047 cm^2) cleaned by using ultrasonic bath with water and isopropanol was used as working electrode. The optimum potential range was determined as -0.7/1.6 V in cyclic voltammetry studies. The polymer (pCoOxim) film obtained by electropolymerization method was washed with DCM to remove any impurities. The scanrate, spectroelectrochemistry and electrochromic studies were accomplished with the obtained polymer film.

For spectroelectrochemical and electrochromic studies, pCoOxim film was accumulated onto ITO surface potentiostatically at different number of cycles (2,4,6 and 8 cycle) in DCM-TBP solvent-electrolyte couple. Iviumstat potentiostat– galvanostat and Agilent 8453 model UV–vis spectrophotometer was combined to analyze opto-electrochemical properties of the polymer film.

Results and Discussion

Spectral analyses

The synthetic route of novel thiohexyl-linked carbazole substituted vicinal dioxime (H_2L) and its cobalt(II) complexes are given at Scheme 1. Novel *vic*-dioxime was prepared by the reaction of 6-(9H-carbazol-9-yl)hexane-1-thiol and cyanogen di-N-oxide, which was prepared from (E, E)-dichloro glyoxime at -15 °C via the coupling reaction. Novel *vic*-dioxime (H_2L) was formed in ca. 44.61% yield as a crystalline product. The structure of H_2L was confirmed with a combination of ^1H, ^{13}C NMR, FT-IR, MS spectral and elemental analysis data (Figure S1, S2, S3, S4). In the ^1H NMR spectrum of compound, there is a triplet concerning –CH_2SH group at δ = 1.32 ppm[38]. After the formation of H_2L, this resonance disappears and a new signal at δ = 2.68 ppm which can be assigned to –CH_2S- moieties belong to the carbazole linked hexyl groups. The novel chemical shifts observed at δ = 9.22 ppm as a singlet after the formation of dioxime is obvious hydroxyimino protons which can be easily identified by deuterium exchange[39]. This singlet indicates an (E, E) isomeric and *S-trans* structure for the vicinal dioxime[40]. This deuterium exchangeable singlet that correspond to equivalent –OH protons also indicate the (E, E)- geometric isomer of dioxime. The desire for coordination with transition metal catios is the (E, E)-isomer since the hydroxyl moieties are directed “outwards” thus enabling the donor atoms lone pair electrons to point “inwards” and coordinate the appropriate metal cations. The other chemical shifts for the, the aromatic protons of the carbazole moieties appeared as singlet at δ = 8.22, dublets at δ = 8.02-7.99, 7.40-7.38 and multiplets at δ = 7.31 and 7.14 ppm in ^1H NMR spectrum of the H_2L. The expectation aliphatic chemical shifts for CH_2 NCH_2, SCH_2 and groups were observed at δ = 1.74, 1.61, 1.46, 1.25 as multiplet and at δ = 4.18, 2.68 ppm as triplet. In the ^{13}C NMR spectrum of dioxime, the new resonances of the azomethine groups was observed at δ = 149.47 ppm and this unique chemical shifts also

View Article Online
DOI: 10.1039/D0NJ03931D

confirmed (E, E) dioxime form. The appearance of novel resonances at 3221 and 1626 cm^{-1} in the FT-IR spectrum of H_2L, concerning with O-H and C=N moieties along with the disappearance of the –SH stretching vibration are in agreement with the proposed structure. The ESI mass spectrum of dioxime exhibits an intense peak at m/z = 650.639 because molecular ion is in accord with the proposed structure. The Co(II) complex of the vic-dioxime was prepared in ca. 96.75% yield by treating cobalt(II) chloride hexahydrate in absolute ethanol with equivalent amount of H_2L in the presence of base (0.10 M KOH in absolute ethanol) at 60 °C under inert atmosphere. A distinct lowering in the pH of the reaction mixture was observed during complexation caused by the deprotonation of the ligand [29,41]. In the FT-IR spectrum of $Co(HL)_2$ complex (Figure S6), the deformation of O-H stretching and weak bending vibrations due to the intra-molecular O-H··O bridge at 1768 cm^{-1} indicate the formation of pseudo macrocycle complexation. The ESI mass spectrum of this complex was the intense peak at m/z = 648.913 confirms loss of the ligand and cobalt moieties (Figure S7). The synthesis of 14-membered macrocyclic BF_2- capped cobalt(II) complex $[Co(LBF_2)_2]$ was performed by adding boron trifluoride diethyl ether and a mixture of dry acetonitrile:dichloromethane solution of the pseudo macrocyclic cobalt(II) complex under argon atmosphere at 45 °C, giving desired macrocyclic complex in ca.72.41% yield. The FT-IR spectrum of this complex (Figure S8) resembles that of the precursor pseudo macrocyclic cobalt(II) complex except for the occurrence of novel characteristic resonances of the BF_2^+ moieties. The presence of the new absorptions at 802 and 1061 cm^{-1} are ascribed to the B-O and B-F vibrations, respectively. The MALDI-TOF mass spectrum of this compound did not exhibit a molecular ion peak; however, peaks at m/z = 1492.275 and 1337.277 were observed (Figure S9). The peaks at m/z = 1492.275 $[M+K]^+$ and the other 1337.277 $[M-BO_3F_3]^+$ could be attributed the proposed structure. It is well known that, the solubility of dioximes and their transition metal complexes in common organic solvents such as chloroform, dichloromethane, diethyl ether are very limited [42–47]. In this study, synthesized dioxime and its BF_2-capped Co(II) complex solubility in organic solvents such as, chloroform, dichloromethane, diethyl ether are exciting features. This result could be attributed the bulky carbazole-linked hexyl chains due to the increase of the lipophilicity of the synthesized compounds [48].

Electrochemical Studies

The Fig. 1 shows cyclic voltammograms of the CoOxim, pCoOxim, H_2L and $p(H_2L)$ at scan rate of 250 mV/s. Onset potential of the CoOxim was observed as 0.59 V during the first cycle of the cyclic voltammetry (Fig 1a). It was observed that the polymer film formed after the onset potential value was reduced at 0.02 and 0.5 V peak potential values during the reverse scan of the first cycle. When analysis of based on the increasing number of cycles, the increase current peak values observed at approximately 0.54 V in each cycle was showed that polymerization actualized on the working electrode surface.

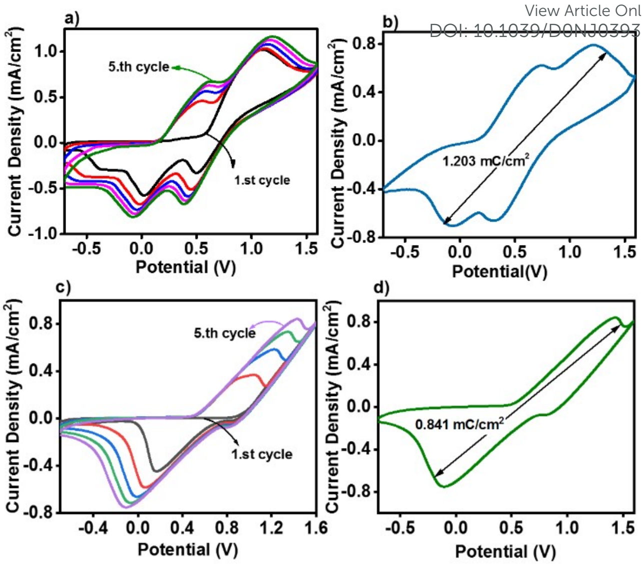

Figure 1 a) Cyclic voltammogram of CoOxim and b) pCoOxim c) Ligand (H_2L) and $P(H_2L)$ in 0.05 M TBP/DCM solution at 250 mV/s.

The charge density of the polymer was calculated as 1.203 mC/cm^2 by integrating the CV graph of the obtained p(Cooxim) polymer (Fig 1b). It was observed that the cv plot of the ligand (H2L) was completely different from that of the Cooxim. While the onset potential of H2L was observed as 0.89 V, the oxidation potential of its polymer was determined as 0.48 V (Fig 1c). It was determined that the charge density of $p(H_2L)$ calculated from the CV graph (Fig 1d) is smaller than that of pCoOxim.

Cyclic voltammogram of the conductive polymer film (Figure 2a) at different scan rates shows that the pCoOxim is electroactive. The nature of the anions in the electrolyte and their diffusion into the polymer film as the counter ions are determine the shape of the redox wave and the kinetics of the electron transfer process. It is also observed from Figure 2a that the oxidation peaks are displaced towards the more positive potential when the scan rate is increased; on the contrary, the reduction peaks are displaced towards the more negative potential. Characteristic of the diffusion-controlled current processes has been observed in redox waves of the CV as it follows linear plot of Ip versus square root of scan rate. (Figure 2 b, c). The reason for the increase in peak separation with increasing scan rate is due to decreasing diffusion layer formed on the working electrode as the scan rate increases. Besides, the Ip_a / Ip_c current rate for this polymer film close to 1 showed that the redox processes were reversible.

Apart from the electrochemical characterizations of the films, FTIR characterizations were carried out. The FTIR spectra of the conductive films obtained as a result of the electropolymerization of the ligand (H2L) and the complex (CoOxim) are given in the ESI as Figure S10. The observation of both peaks at 802 and 1063 cm^{-1} which ascribed to the B-O and B-F vibrations in the FTIR spectrum of the pCoOxim polymer film shows caged metal centers remains intact after electropolymerization of the CoOxim.

View Article Online
DOI: 10.1039/D0NJ03931D

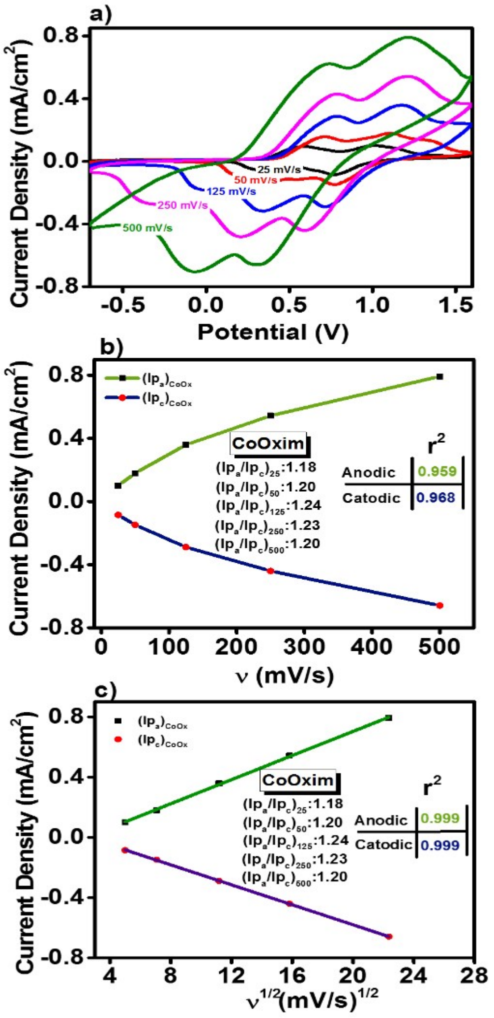

Figure 2 a) Cyclic voltammetry graphs of the pCoOxim polymer film at different scan rates, b) scan rate-peak current density graphs of the pCoOxim polymer film, c) the redox peak current vs. square root of scan rates of the pCoOxim polymer film

Redox stability of conductive polymers is one of the most important requirements for their ultimate applications. Due to environmental conditions and repetitive potential applications, there may be failures in the redox stability of conductive polymers. Usually, different potentials are applied to the polymers for a long time with repetitive cyclic voltammetry technique at determined scanning rate to examine the redox stability of conductive polymers in monomer free solution. Long-term redox stability of pCoOxim film in monomer free solution at scan-rate of 250 mV/s has been shown in Figure 3. As a result of the redox stability test performed for pCoOxim, only 16.1 percent loss was observed from the initial charge density value. This study revealed that synthesized polymer film with caged metal centers has excellent electrochemical and optical stability.[49–55]

Spectroelectrochemical Studies

In all practical applications using thin films, thickness optimization is very important as the film thickness affects properties of the material such as optical and electrical properties. Since the film thickness can easily be adjusted in electrochemical techniques, film thickness optimization was carried out by changing the number of scan in cyclic voltammetry technique. For this purpose, conductive polymer films with different thickness were obtained on the ITO electrode by applying a different number of cycles (2, 4, 6, 8, 10 cycles) in cyclic voltammetry and their spectrochemical properties were examined. After the analysis of the spectroelectrochemical curves, it has been observed that pCoOxim film at reduced state showed an absorption bands with maximum at 305, 315, 308, 305 and 309 nm assigned to the π-π* electronic transition respectively for each study (2, 4, 6, 8, 10 cycles) (Figure 4). The absorption between 300-315 nm is thought to belong to the π-π* transitions of polycarbazole derivatives. Noteworthy, as the number of cycles changed, the energetic state of the polymer has changed with the arising of a broad absorption band at the low energy side of the spectra. This band is thought to be due to the corresponds to the appearance of new energy levels inside the band gap during the doping process depending on the amount of polymer that differs. When the applied potential value reached 1.4 V, a significant change was observed in the region where bipolaron bands were formed.

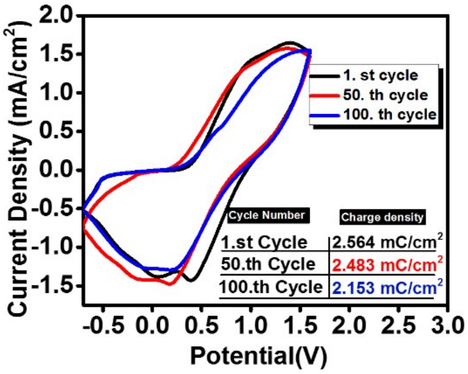

Figure 3 . Long term stability of pCoOxim film in monomer free solution at scan-rate of 250 mV/s.

Besides, the absorptions between 658-665 nm belongs the bipolaron band absorptions of the polymeric film[56]. While the location of these bands are maintained with the increasing potential its intensity its density varied depending on the number of cycles. The highest absorption value was observed in polymer film coated with 4 cycles. Also, the electrochromic colors and corresponding CIELAB color space values of PCoOxim film have been shown in Figure 5. As the applied potential increases, the pCoOxim film showed a gradual color changing starting from bleached (undoped) to green (doped). For comparison, the spectroelectrochemistry plot of p (H2L) is given in ESI as Figure S11)

View Article Online
DOI: 10.1039/D0NJ03931D

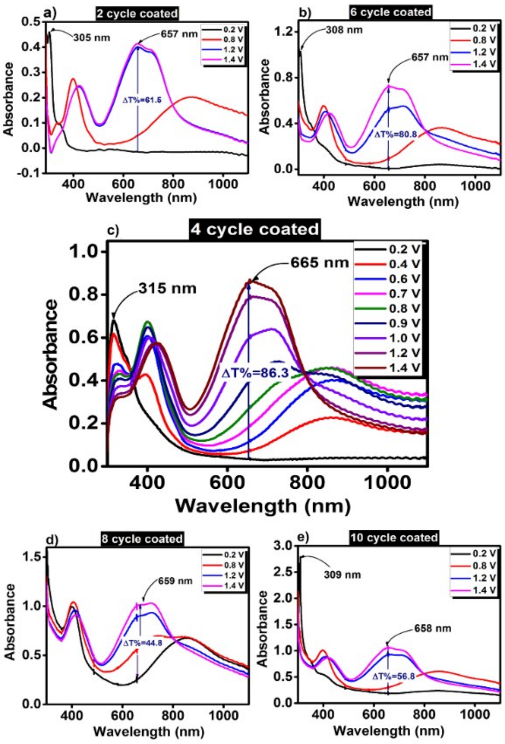

Figure 4 Spectroelectrochemical investigations of the pCoOxim polymer films coated with a) 2 cycles, b) 6 cycles, c) 4 cycles, d) 8 cycles and e) 10 cycles.

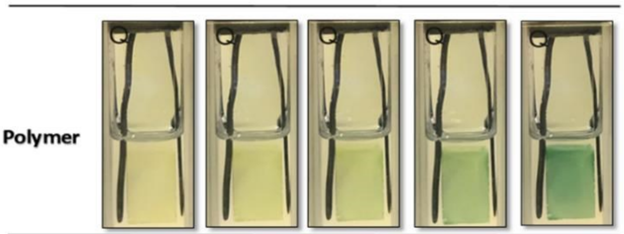

L*	93	78	77	63	48
a*	-2	-7	-10	-20	-15
b*	20	35	44	31	26

Figure 5 Electrochromic colors of the pCoOxim film when applied different potentials

Electrochromism is the ability to switch between the reduced and oxidized states of polymeric films, which allows the conductive polymer to be used in many applications. The square-wave potential step is usually applied to evaluate the electrochromic switching properties of CPs. The most important factors affecting the electrochromic switching time of conductive polymers are film morphology, electrolyte type, and the penetration of ions into electroactive centers. For this reason, in order to evaluate the reversibility process, the polymer film was switched between its' reduction and oxidation potential in monomer free solution (Figure 6). When the optical contrast values of the materials were compared, it was found that the polymer obtained by coating with 4 cycles had the highest value. This is thought to be related to the change in semi-conductivity depending on the coating amount of the polymer. Also, the Figure 8, represent the transmittance at the maximum wavelength for colored and bleached states. The data of the spectroelectrochemical and electrochromic study are summarized in Table 1.

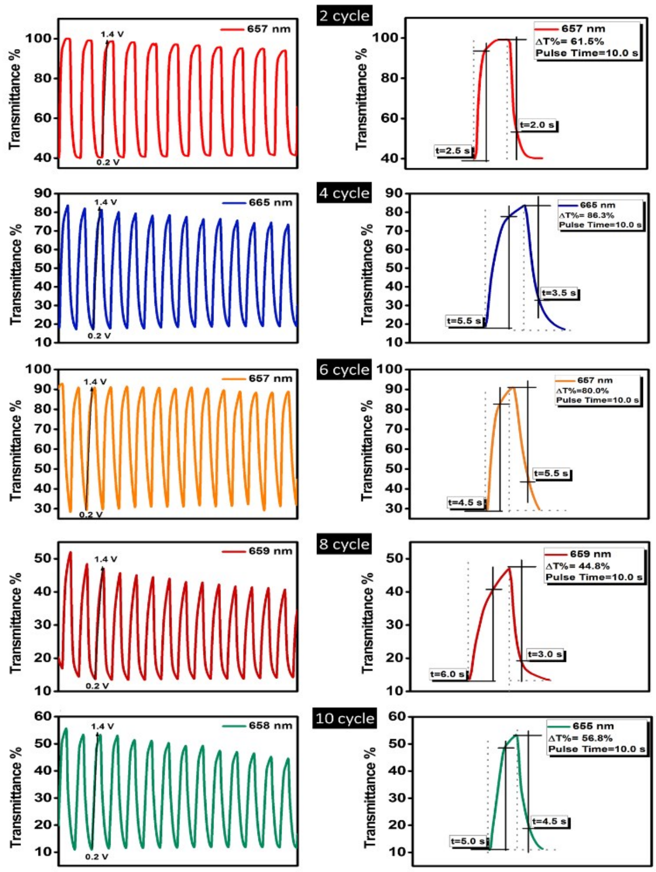

Figure 6 Long-term chronoabsormetry investigation for polymer synthesized in different cycle numbers in cyclic voltammetry at 250 mV/s.

Optical contrast values in the reduction and oxidation states of conductive polymer films obtained different cycle numbers during CV studies were plotted to determine highest optical contrast value for specific thickness. It was seen that in Fig 7, as the film thickness increases, the optical contrast values of the colored and bleached states of the conductive polymer tend to decrease. It was determined form Fig 7 that the highest optical contrast value belongs to the conductive polymer obtained by cycle number of 4.

When the literature analyzed within the scope of this study, it has been determined that studies on oximes are very limited. It is therefore very difficult to make a comparison. For comparison, metal and carbazole containing polymers were researched and the comparison table (Table 2) is given below.

View Article Online
DOI: 10.1039/D0NJ03931D

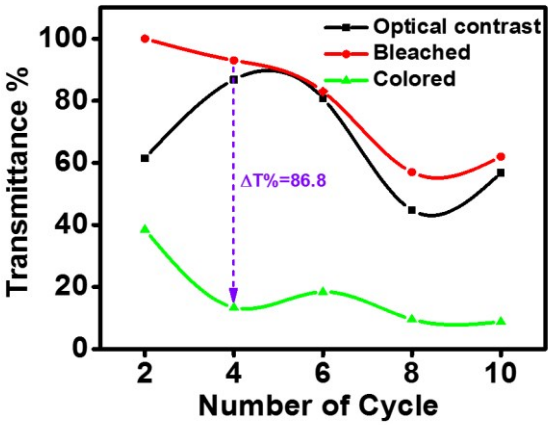

Figure 7 Graph of transmittance at coloured and bleached states

Table 1 Electrochemical and optical properties of the pCoOxim

pCoOxim Cycle Number	Band Gap (eV)	%ΔT Optical Contrast	Switching Time (s)
2 cycle	3.68	81.6	2.5
4 cycle	2.86	86.8	5.5
6 cycle	3.66	80.0	4.5
8 cycle	3.68	44.8	6.0
10 cycle	3.87	56.8	5.0

Table 2 Comparison of electrochromicl performance of metallopolymer.

Polymer	ΔT%	Switching Time (s)	References
P(ZnPc)	53	6.8	57
P(n-ZnPc)	70.5	5.0	58
CuPc-PANI	58	1.96	59
CoPc	1.5	0.9	60
Mn(Cl)Pc	4.0	1.0	
Fe(Cl)Pc	7.0	2.9	
Sn(Cl)2Pc	16.0	7.0	
pCoOxim	**86.8**	**5.5**	**Our work**

EQCM Studies

Piezoelectric micro-gravimetry using quartz crystal microbalance (QCM) to monitor mass change with nano-gram sensitivity is a very useful technique that can be applied to many areas such as sensor applications, reaction mechanisms and material structure change investigation. QCM technique is based on the mechanical oscillation of the piezoelectric material when exposed to an AC potential and the frequency change of the oscillation of the piezoelectric material is associated with mass change on the quartz crystal surface. By coupling electrochemistry (EQCM), electrochemical reaction mechanisms can be revealed by comparing the mass changes on the crystal surface with the increased or consumed charge change from the redox transformations. Detailed information about the relative contribution of different anions and cations in electrochemical processes and the rate of the mass transport processes can be obtained with the EQCM technique[61,62]. This technique is of particular importance in the investigation of the synthesis and electrochemical behavior of conductive polymers. Recently, EQCM technique has made great contributions to the analysis of the growth mechanism in synthesis, doping-dedoping process and charge transfer properties of conductive polymers. For this purpose, the electropolymerization of the CoOxim monomer and the redox behavior of its conductive polymer (pCoOxim) have been examined with the EQCM technique.

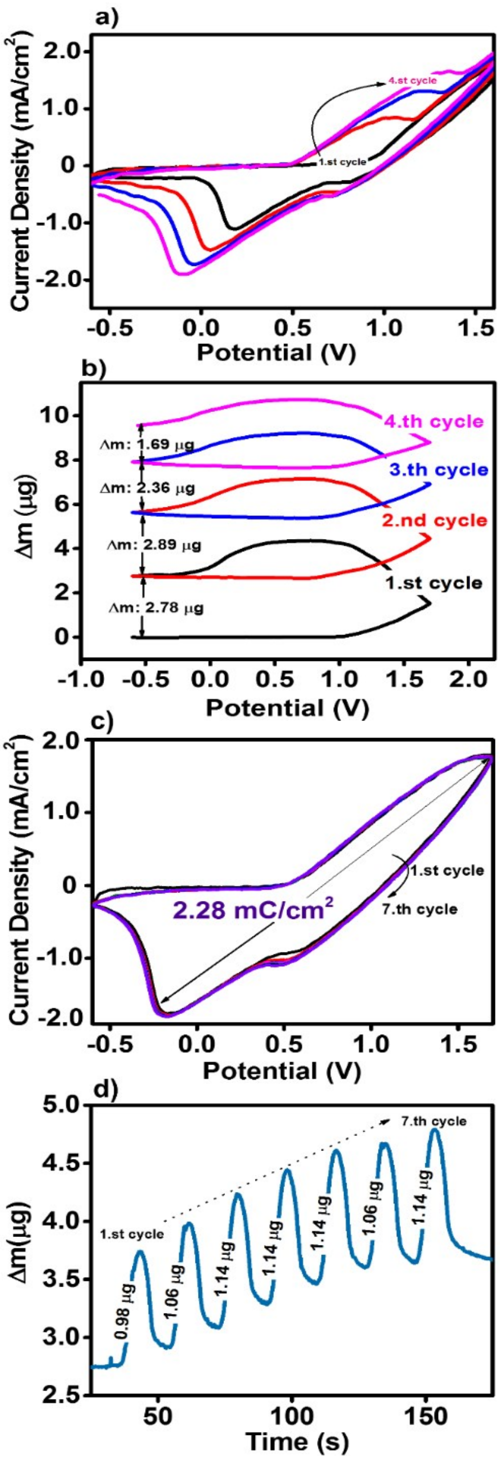

Figure 8 Cyclic voltammetric deposition of pCoOxim from a solution of 0.001 M CoOxim and 0.05 M TBP/DCM and b) Simultaneously recorded mass-potential plot. Working electrode: 10 MHz quartz crystals c) Cyclic voltammogram of 0.001 M pCoOxim and d)

View Article Online
DOI: 10.1039/D0NJ03931D

The mass-time graph of pCoOxim polymer in monomer free solution at 250 mV/s scan rate.

Figure 8 shows the cyclic voltammogram and EQCM responses to the cyclic voltammetric deposition of pCoOxim at a scan rate of 250 mV/s in dichloromethane (DCM) solution consist of 0.001 M CoOxim monomer and 0.05 M Tetrabutylammonium hexafluorophosphate (TBP). Cooxim monomer is electro-oxidized at potentials positive of about 1.0 V in the first positive sweep and the simultaneous mass increase at the EQCM demonstrates the onset potential of the pCoOxim deposition on the electrode. Since monomer oxidation continues, mass increase proceeds until the onset potential value is reached in reverse scan of the CV. Whereas the mass is remains constant over a certain potential range after the onset potential value, a decrease is observed after the reduction potential value of the polymer formed. The reason for the mass decrease can be considered as the supporting electrolyte and solvent that removed from reduced polymer structure. When each cycle was analyzed separately, it was revealed that the amount of pCoOxim coated on the electrode decreased as the number of cycles increased. This result can be explained by the fact that the working electrode has higher conductivity than the coated polymer. The polymer mass coated on the electrode in each cycle has been calculated and written on the Fig 8b graph. After the EQCM characterization of the electrochemical polymerization process, redox properties of conductive polymer film obtained on the EQCM electrode has been investigated in the monomer free electrolyte solution. When mass changes in repetitive cyclic voltammetry in the electrolyte solution of the polymer film have been examined by the EQCM technique, it has been seen that the mass changes remain approximately constant (Fig.9). This mass change, approximately 1.14 µg, corresponds to dopant anions taken into and removed from the polymer structure as a result of the redox process of the conductive polymer. These studies revealed that synthesized polymer film with caged metal centers has excellent electrochemical and optical stability.

Conclusions

In this study conductive metallopolymer with caged metal centers was synthesized with a synergistic combination of metal centers and conducting polymers to desired optical and electrical properties of the material for ultimate applications. For this purpose, first of all the novel S,S'-substituted vicinal dithioglyoxime has been synthesized from 6-(9H-carbazol-9-yl)hexane-1-thiol and cyanogen di-N-oxide, which was prepared from (E, E)-dichloro glyoxime at -15 °C. Mononuclear cobalt(II) complex of dioxime with a metal:ligand ratio of 1:2 was isolated and this pseudo macrocyclic Co(II) complex has been converted to full macrocycle by replacement of the hydrogen atoms with $+BF_2$ moieties which act as strong electron-withdrawing units to enhance stability of the transition metal and to increase solubility of the macrocycle in common organic solvents. After electrochemical polymerization polycarbazole based conductive metallopolymer with caged metal centers have been obtained. As a result of the optical and electrochemical characterization of the unique structure, the highest optical contrast value was obtained among the polycarbazole derivatives in the literature. Electrochemical polymerization and electrochemical properties of the conducting metallopolymer have been also investigated with EQCM studies. Thanks to the superior properties of this unique organic-inorganic hybrid structure obtained with simple organic reactions, it is obvious that it will have the great potential to be used in numerous applications such as smart windows, sensor applications, OLED etc.

Conflicts of interest

There are no conflicts to declare.

Notes and references

1 B. Fabre, E. Hao, Z. M. LeJeune, E. K. Amuhaya, F. Barrière, J. C. Garno and M. G. H. Vicente, *ACS Appl. Mater. Interfaces*, 2010, **2**, 691–702.
2 T. W. Hesterberg, X. Yang and B. J. Holliday, *Polyhedron*, 2010, **29**, 110–115.
3 B. J. Holliday and T. M. Swager, *Chem. Commun.*, 2005, 23.
4 G. K. Çılgı, M. Karakuş and M. Ak, *Synth. Met.*, 2013, **180**, 25–31.
5 Y. Liang, D. Strohecker, V. Lynch, B. J. Holliday and R. A. Jones, *ACS Appl. Mater. Interfaces*, 2016, **8**, 34568–34580.
6 T. Soganci, D. O. Demirkol, M. Ak and S. Timur, *RSC Adv.*, 2014, **4**, 46357–46362.
7 S. Soyleyici, M. Karakus and M. Ak, *J. Electrochem. Soc.*, 2016, **163**, H679–H683.
8 R. Ayranci, D. Demirkol, M. Ak and S. Timur, *Sensors*, 2015, **15**, 1389–1403.
9 T. Soganci, M. Ak, S. Ocal and M. Karakus, *J. Inorg. Organomet. Polym. Mater.*, 2015.
10 R. C. Smith, A. G. Tennyson, A. C. Won and S. J. Lippard, *Inorg. Chem.*, 2006, **45**, 9367–9373.
11 T. Y. Tekbaşoğlu, T. Soganci, M. Ak, A. Koca and M. K. Şener, *Biosens. Bioelectron.*, 2017.
12 R. Ayranci, M. Ak, S. Ocal and M. Karakus, *Des. Monomers Polym.*, 2016, **19**, 429–436.
13 Ö. Göktuğ, T. Soganci, M. Ak and M. K. Şener, *New J. Chem.*, 2017, **41**, 14080–14087.
14 M. A. Said, T. Soganci, M. Karakus and M. Ak, *J. Organomet. Chem.*, 2017, **851**, 248–253.
15 R. Back and R. B. Lennox, *Langmuir*, 1992, **8**, 959–964.
16 R. Ayranci, M. Ak, M. Karakus and H. Cetisli, *Des. Monomers Polym.*, 2016, **19**, 545–552.
17 P. Camurlu, Z. Bicil, C. Gültekin and N. Karagoren, *Electrochim. Acta*, 2012, **63**, 245–250.
18 T. Soganci, Y. Baygu, N. Kabay, Y. Gök and M. Ak, *ACS Appl. Mater. Interfaces*, 2018, **10**, 21654–21665.
19 R. Olgac, T. Soganci, Y. Baygu, Y. Gök and M. Ak, 2017, **98**, 202–209.

View Article Online
DOI: 10.1039/D0NJ03931D

20 D. A. Weinberger, T. B. Higgins, C. A. Mirkin, C. L. Stern, L. M. Liable-Sands and A. L. Rheingold, *J. Am. Chem. Soc.*, 2001, **123**, 2503–2516.

21 N. Guven, H. Sultanova, B. Ozer, B. Yucel and P. Camurlu, *Electrochim. Acta*, 2020.

22 D. A. Weinberger, T. B. Higgins, C. A. Mirkin, L. M. Liable-Sands and A. L. Rheingold, *Angew. Chemie Int. Ed.*, 1999, **38**, 2565–2568.

23 J. L. Reddinger and J. R. Reynolds, *Chem. Mater.*, 1998, **10**, 1236–1243.

24 S. S. Zhu and T. M. Swager, *J. Am. Chem. Soc.*, 1997, **119**, 12568–12577.

25 Y. Voloshin, I. Belaya and R. Krämer, *Cage Metal Complexes*, Springer International Publishing, Cham, 2017.

26 G. N. Schrauzer, *Chem. Ber.*, 1962, **95**, 1438–1445.

27 P. Connolly and J. H. Espenson, *Inorg. Chem.*, 1986, **25**, 2684–2688.

28 A. S. Abusamleh, P. J. Chmielewski, P. R. Warburton, L. Morales, N. A. Stephenson and D. H. Busch, *J. Coord. Chem.*, 1991, **23**, 91–111.

29 H. Basri, *Online*, 2001, **5**, 364–368.

30 J. Wang, C. Li, Q. Zhou, W. Wang, Y. Hou, B. Zhang and X. Wang, *Dalt. Trans.*, 2015, **44**, 17704–17711.

31 A. Fihri, V. Artero, M. Razavet, C. Baffert, W. Leibl and M. Fontecave, *Angew. Chemie - Int. Ed.*, 2008, **47**, 564–567.

32 L. M. Hansen, P. N. V. P. Kumar and D. S. Marynick, *Inorg. Chem.*, 1994, **33**, 728–735.

33 V. Alexander and V. V. Ramanujam, *Inorganica Chim. Acta*, 1989, **156**, 125–137.

34 A. Chakravorty, *Coord. Chem. Rev.*, 1974, **13**, 1–46.

35 S. Serin, Y. Gök, S. Karaböcek and N. Gültekin, *Analyst*, 1994, **119**, 1629–1631.

36 K. A. Lance, K. A. Goldsby and D. H. Busch, *Inorg. Chem.*, 1990, **29**, 4537–4544.

37 V. C. G. I, V. Mini, J. M. Dean, H. Frommeld, M. Institut and P. Pa, 1965, **2077**.

38 T. Soganci, M. Ak, S. Ocal and M. Karakus, *J. Inorg. Organomet. Polym. Mater.*, 2015, 1011–1018.

39 G. Dutta, K. Kumar and B. D. Gupta, *Organometallics*, 2009, **28**, 3485–3491.

40 V. Ahsen, A. Gürek, A. Gül and Ö. Bekâroğlu, *J. Chem. Soc., Dalt. Trans.*, 1990, 5–8.

41 H. Kantekin, Ö. Hasançebi, R. Abbasoglu and Y. Gök, *New J. Chem.*, 2001, **25**, 879–886.

42 V. Ahsen, A. Gurek, A. Gul and O. Bekiiroalu, 1990, 13–16.

43 Y. Gök and Y. Atalay, *J. Incl. Phenom. Mol. Recognit. Chem.*, 1997, **28**, 287–298.

44 D. Mendil, A. Bilgin, Y. Gök and H. B. Şentürk, *J. Incl. Phenom.*, 2002, **43**, 265–270.

45 E. Musluoğlu and Ö. Bekâroglu, *J. Coord. Chem.*, 1996, **39**, 253–264.

46 E. Hamuryudan and Öz. Bekaroğlu, *Chem. Ber.*, 1994, **127**, 2483–2488.

47 M. Ertas, V. Ahsen, A. Gül and Ö. Bekâroğlu, *J. Organomet. Chem.*, 1987, **335**, 105–108.

48 I. Gürol, V. Ahsen and Ö. Bekâroğlu, *J. Chem. Soc. Dalt. Trans.*, 1992, 2283–2286.

49 G. Bagdžiūnas, Š. Žukauskas and A. Ramanavičius, *Biosens. Bioelectron.*, 2018, **102**, 449–455.

50 Š. Žukauskas, A. Ramanavičius and G. Bagdžiūnas, *J. Electrochem. Soc.*, 2019, **166**, B316–B321.

51 G. Bagdžiūnas, D. Palinauskas and A. Ramanavičius, *Dye. Pigment.*, 2020, **177**.

52 S. V. Dudkin, A. S. Belov, Y. V. Nelyubina, A. V. Savchuk, A. A. Pavlov, V. V. Novikov and Y. Z. Voloshin, *New J. Chem.*, 2017, **41**, 3251–3259.

53 Y. Z. Voloshin, O. A. Varzatskii, A. S. Belov, Z. A. Starikova, A. V. Dolganov, V. V. Novikov and Y. N. Bubnov, *Inorganica Chim. Acta*, 2011, **370**, 322–332.

54 Y. Z. Voloshin, A. V. Dolganov, O. A. Varzatskii and Y. N. Bubnov, *Chem. Commun.*, 2011, **47**, 7737–7739.

55 W. Liu, W. Huang, C. H. Chen, M. Pink and D. Lee, *Chem. Mater.*, 2012, **24**, 3650–3658.

56 E. Karatas, M. Guzel and M. Ak, *J. Electrochem. Soc.* , 2017, **164** , H463–H469.

57 R. Olgac, T. Soganci, Y. Baygu, Y. Gök and M. Ak, *Biosens. Bioelectron.*, 2017, **98**, 202–209.

58 T. Soganci, Y. Baygu, N. Kabay, Y. Gök and M. Ak, *ACS Appl. Mater. Interfaces*, 2018, **10**, 21654–21665.

59 M. Ouyang, X. Hu, X. Shao, L. Chen, W. Li, R. Bai, L. Zhang, X. Lv, A. Tameev and C. Zhang, *RSC Adv.*, 2019, **9**, 34382–34388.

60 E. B. Orman, Z. Odabaş and A. Rıza Özkaya, *J. Electrochem. Soc.*, 2018, **165**, H530–H548.

61 D. Plausinaitis, L. Sinkevicius, U. Samukaite-Bubniene, V. Ratautaite and A. Ramanavicius, *Talanta*, 2020, **220**, 121414.

62 D. Plausinaitis, L. Sinkevicius, L. Mikoliunaite, V. Plausinaitiene, A. Ramanaviciene and A. Ramanavicius, *Phys. Chem. Chem. Phys.*, 2017, **19**, 1029–1038.

View Article Online
DOI: 10.1039/D0NJ03931D

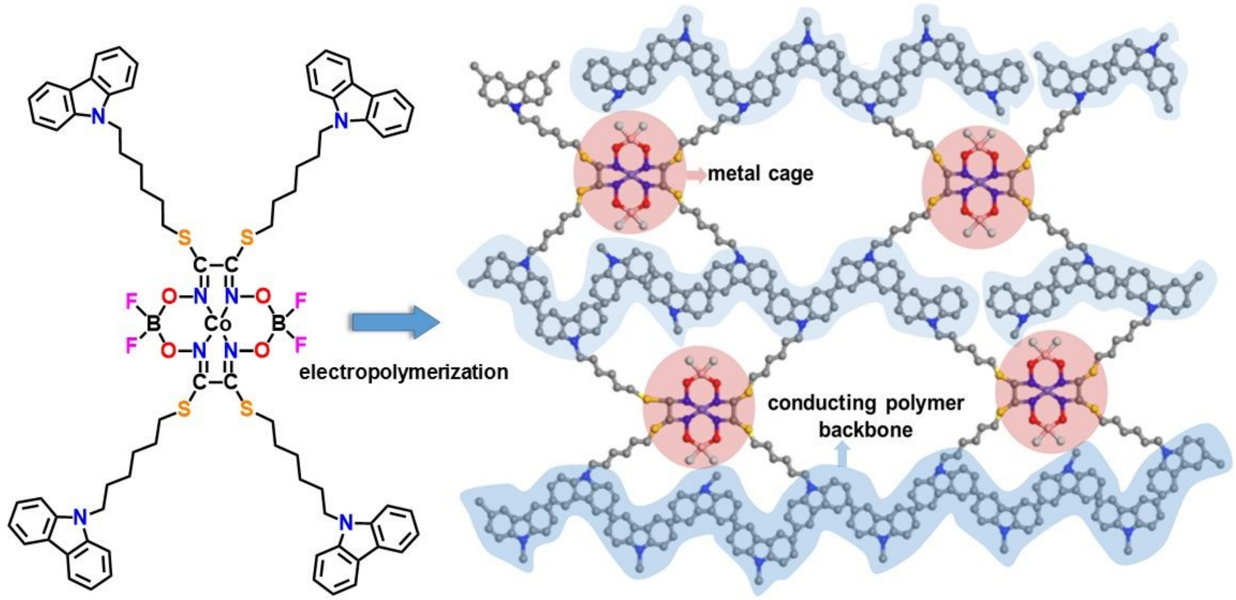

Polycarbazole based conductive metallopolymer with caged metal centers have been obtained. As a result of the optical and electrochemical characterization of the unique structure, the highest optical contrast value was obtained among the polycarbazole derivatives.